Contribution from the Department of Chemistry and Biochemistry, University of Colorado, Boulder, Colorado 80309

Coordination Oligomers and a Coordination Polymer of Zinc Tetraarylporphyrins

Everly B. Fleischer*,† and Amy M. Shachter

Received January 3, 1991

The structure of (5-pyridyl-10,15,20-triphenylporphyrinato)zinc(II) ($C_{43}H_{27}N_5Zn$) was determined by visible spectroscopy, proton NMR spectroscopy, fluorescence spectrophotometry, and X-ray crystallography. Spectroscopic results indicated that the pyridine on the porphyrin periphery was bound to the metal center of an adjacent porphyrin, thereby creating a polymer. The crystal structure of the ZnMPyTPP polymer revealed that the polymer was in a long chain, zigzag conformation with an unusual 25° tilt of the pyridine ring. The polymer crystallized in the monoclinic space group $P2_1/c$ with a = 10.839 (3) Å, b = 19.124 (9) Å, c = 16.158 (6) Å, β = 90.32 (3)°, and Z = 4. For 2130 observed reflections, the refinement yielded R = 0.0626. The structure of the polymer in solution was shown to be similar to that in the solid state by NMR porphyrin ring current theory. Coordinated dimers and trimers were formed by the coordination of 5-pyridyl-10,15,20-triphenylporphyrin, 5,10-dipyridyl-15,20-diphenylporphyrin, or 5,15-dipyridyl-10,20-diphenylporphyrin with (5,10,15,20-tetraphenylporphyrinato)zinc(II) and were characterized by spectroscopic methods.

Oligomers and polymers of metalloporphyrins have been of interest for many years. Linked porphyrin dimers have been studied as models for the photosynthetic "special pair",[1] as electrocatalysts for the activation of small molecules,[2] and as photodynamic antitumor agents.[3] Polymer-bound porphyrins have been investigated as hemoglobin models[4] and as hetereogeneous catalysts.[5] Additionally, systems with porphyrins as a monomeric unit of the polymer have been studied. For example, tetraarylporphyrin derivatives have been copolymerized with acrylic acid and a quinone derivative to form a polymer with a structured porphyrin–quinone orientation designed to model photosynthesis.[6] Tsuchida and co-workers synthesized an iron porphyrin–phospholipid copolymer that was designed to transport oxygen and that displayed oxygen binding affinities similar to that of hemoglobin.[7] Furthermore, electropolymerization of porphyrins has recently been explored by several groups as a method of forming thin polymeric films on electrodes for electrocatalysis.[8] The photoactivity of thin polymeric porphyrin films has also been explored.[9]

Metalloporphyrin polymers, where the polymer linkage is formed by a bridging ligand, have been studied. Linear polymers that involve iron, ruthenium, and osmium metalloporphyrins joined by bridging ligands such as pyrazine demonstrated interesting conductivity, with the electrons flowing along the metal–pyrazine polymeric backbone.[10]

One area of metalloporphyrin chemistry that has received little attention but may lead to systems of interesting structural and electronic properties is that of coordination polymers. In these systems, the polymer is formed by multifunctional porphyrin monomers that coordinate to metal ions through the porphyrin pyrrole nitrogens, as well as through substituents on the porphyrin periphery. The oligomers and polymers are propagated by the coordination of the peripheral substituent to the metal center of an adjacent porphyrin.

The X-ray structure of polymeric (5,10,15,20-tetrakis(*o*-nicotinamidophenyl)porphyrinato)iron(III) was determined by Gunter and co-workers.[11] The structure showed that the polymeric linkage was formed by the coordination of the nicotine nitrogen of one porphyrin to the metal center of an adjacent porphyrin forming a coordinated polymer. This polymer was the only reported structure of a coordinated porphyrin polymer until this study.[12]

We report the synthesis and characterization of a simple dimer composed of (5,10,15,20-tetraphenylporphyrinato)zinc(II) (ZnTPP) and 5-pyridyl-5,10,15,20-triphenylporphyrin, two distinct trimers consisting of ZnTPP and 5,10-dipyridyl-15,20-diphenylporphyrin, or 5,15-dipyridyl-10,20-diphenylporphyrin and a (5-monopyridyl-10,15,20-triphenylphorphyrinato)zinc(II) polymer.

† Presently at the Chemistry Department, University of California, Riverside, CA 92521.

(1) (a) Dolphin, D.; Hiom, J.; Paine, J. B. *Heterocycles* **1981**, *16*, 417. (b) Boxer, S. G. *Biochem. Biophys. Acta* **1983**, *726*, 265. (c) Wasielewski, M. R. *Photochem. Photobiol.* **1988**, *47*, 923. (d) Sessler, J. L.; Johnson, M. R.; Lin, T.; Creager, S. E. *J. Am. Chem. Soc.* **1988**, *110*, 3659, and references therein.

(2) (a) Chang, C. K.; Abdalmuhdi, I. *J. Org. Chem.* **1983**, *48*, 5388. (b) Chang, C. K.; Fillers, J. P.; Ravichandran, A.; Abdalmuhdi, I.; Tulinsky, A. *J. Am. Chem. Soc.* **1986**, *108*, 417. (c) Ni, C.; Abdalmuhdi, I.; Chang, C. K.; Anson, F. C. *J. Phys. Chem.* **1987**, *91*, 1158. (d) Collman, J. P.; Chong, A. O.; Jameson, G. B.; Oakley, R. T.; Rose, E.; Schmittoy, E. R.; Ibers, J. A. *J. Am. Chem. Soc.* **1981**, *103*, 516. (e) Collman, J. P.; Anson, F. C.; Barnes, C. E.; Bencosme, C. S.; Geiger, T.; Evitt, E. R.; Kreh, R. P.; Meier, K.; Pettman, R. B. *J. Am. Chem. Soc.* **1983**, *105*, 2695. (e) Collman, J. P.; Bencosme, C. S.; Durand, R. R.; Kreh, R. P.; Anson, F. C. *J. Am. Chem. Soc.* **1983**, *105*, 2699. (f) Collman, J. P.; Bencosme, C. S.; Barnes, C. E.; Miller, B. D. *J. Am. Chem. Soc.* **1983**, *105*, 2704. (g) Collman, J. P.; Kim, K.; Ibers, J. *J. Am. Chem. Soc.* **1988**, *110*, 4242. (h) Collman, J. P.; Hendricks, N. H.; Leidner, C. R.; Ngameni, E.; L'Her, M. *Inorg. Chem.* **1988**, *27*, 387. (i) Cowan, J. A.; Sanders, J. K. M. *J. Chem. Soc., Chem. Commun.* **1985**, 1214. (j) Neuman, K. H.; Vogtle, F. *J. Chem. Soc., Chem. Commun.* **1988**, 520. (k) Hunter, C. A.; Meah, M. N.; Sanders, J. K. M. *J. Chem. Soc. Chem. Commun.* **1988**, 692. (l) Anderson, H. L.; Hunter, C. A.; Sanders, J. K. M. *J. Chem. Soc., Chem. Commun.* **1989**, 226.

(3) (a) Scourides, P. A.; Bohmer, R. M.; Kaye, A. H.; Morstyn, G. *Cancer Res.* **1987**, *47*, 3439. (b) Morris, I. K.; Ward, A. D. *Tetrahedron Lett.* **1988**, *29*, 2501.

(4) (a) Wang, J. H.; Brinigar, W. S. *Proc. Natl. Acad. Sci. U.S.A.* **1960**, *46*, 958. (b) Tsuchida, E.; Nishide, H. *Top. Curr. Chem.* **1986**, *32*, 63.

(5) Takemoto, K.; Inaki, Y.; Ottenbrite, R. M. *Functional Monomers and Polymers*; Marcel Dekker, Inc.: New York, 1987.

(6) Guillet, J. E.; Takahaski, Y.; McIntosh, M.; Bottem, J. R. *Macromolecules* **1985**, *18*, 1788.

(7) (a) Tsuchida, E.; Nishide, H.; Yuasa, M.; Babe, T.; Fukuzumi, M. *Macromolecules* **1989**, *22*, 66. (b) Tsuchida, E.; Nishida, H.; Yuasa, M.; Hashimoto, Y. *Macromolecules* **1987**, *20*, 461.

(8) (a) Macor, K. A.; Su, Y. O.; Miller, L. A.; Spiro, T. G. *Inorg. Chem.* **1987**, *26*, 2594. (b) Bettleheim, A.; White, B. A.; Raybuck, S. A.; Murray, R. W. *Inorg. Chem.* **1987**, *26*, 1009.

(9) Wamser, C. C.; Bard, R. R.; Senthilathipan, V.; Anderson, V. C.; Yates, J. A.; Lonsdale, H. K.; Rayfield, G. W.; Friesen, D. T.; Lorenz, D. A.; Stangle, G. C.; van Eikeren, P.; Baer, D. R.; Ransdell, R. A.; Golbeck, J. H.; Babcock, W. C.; Sandberg, J. J.; Clarke, S. E. *J. Am. Chem. Soc.* **1989**, *111*, 8485.

(10) (a) Collman, J. P.; McDevitt, J. T.; Yee, G. T.; Leidner, C. R.; McCullough, L. G.; Little, W. A.; Torrance, J. B. *Proc. Nat. Acad. Sci. U.S.A.* **1986**, *83*, 4581. (b) Maldotti, A.; Varani, G.; Amadelli, R.; Bartocci, C. *New. J. Chem.* **1988**, *12*, 819. (c) Zhukhovitskii, V. B.; Khidekel, M. L.; Dyumaev, K. M. *Russ. Chem. Rev. (Engl. Transl.)* **1985**, *54*, 144. (d) Liou, K.; Ogawa, M. Y.; Newcomb, T. P.; Quirion, G.; Lee, M.; Poirier, M.; Halperin, W. P.; Hoffman, B. M.; Ibers, J. A. *Inorg. Chem.* **1989**, *28*, 3889.

(11) Gunter, M. J.; McLaughlin, G. M.; Berry, K. J.; Murry, K. S.; Irving, M.; Clark, P. E. *Inorg. Chem.* **1984**, *23*, 283.

(12) Shachter, A. M.; Fleischer, E. B.; Haltiwanger, R. C. *J. Chem. Soc., Chem. Commun.* **1988**, 960.

0020-1669/91/1330-3763$02.50/0

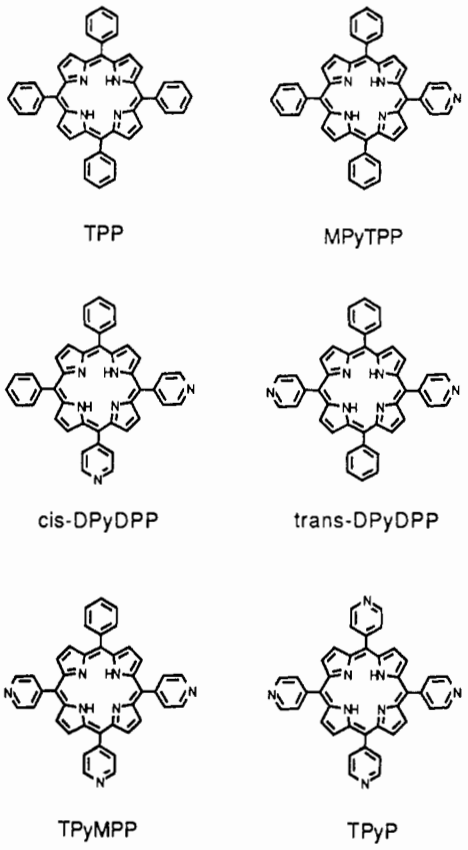

Figure 1. Six porphyrin isomers.

Experimental Section

Synthesis and Purification of Porphyrin Monomers. All chemicals were reagent grade unless otherwise specified. The porphyrin monomers were prepared according to standard literature methods.[13] Pyrrole (7.0 mL, 100 mmol), benzaldehyde (7.5 mL, 74 mmol), and 4-pyridinecarboxaldehyde (2.5 mL, 26 mmol) were refluxed in 250 mL of 99% propionic acid for 1 h. The reaction mixture was then cooled and allowed to stand overnight. Filtration and methanol washing afforded 2.07 g (13% yield) of a purple crystalline product. The product was analyzed by silica gel thin layer chromatography and found to be a mixture of the six possible porphyrin isomers: 5,10,15,20-tetraphenylporphyrin (TPP), 5-pyridyl-10,15,20-triphenylporphyrin (MPyTPP), 5,10-dipyridyl-15,20-diphenylporphyrin (*cis*-DPyDPP), 5,15-dipyridyl-10,20-diphenylporphyrin (*trans*-DPyDPP), 5,10,15-tripyridyl-20-phenylporphyrin (TPyMPP), and 5,10,15,20-tetrapyridylporphyrin (TPyP) (Figure 1). The R_f values of the isomers were 0.88 (TPP), 0.60 (MPyTPP), 0.42 (*trans*-DPyDPP), 0.22 (*cis*-DPyDPP), 0.12 (TPyMPP), and 0.08 (TPyP) in 98% chloroform/2% ethanol. The R_f values were assigned according to literature values.[14]

The isomers were separated by using flash chromatography with silica gel and a chloroform/ethanol solvent system consisting initially of 98% chloroform/2% ethanol and gradually ending with 100% ethanol. Upon separation, the product mixture consisted of 30% TPP, 20% MPyTPP, 2% *trans*-DPyDPP, 8% *cis*-DPyDPP, 15% TPyMPP, 25% TPyP. The identities of MPyTPP, *cis*- and *trans*-DPyDPP, and TPyMPP were confirmed by elemental analysis, visible spectroscopy, and NMR spectroscopy.

MPyTPP [$C_{43}N_5H_{29}\cdot{}^1/_2H_2O$; fw = 624.74 g/mol]. Anal. Calcd: C, 82.67; N, 11.21; H, 4.84; O, 1.28. Found: C, 82.61; N, 11.11; H, 4.61; O, 1.39. Visible spectrum [λ, nm, in $CHCl_3$ ($\epsilon \times 10^4$, cm^{-1} M^{-1})]: 418 (25), 516 (1.7), 550 (0.7), 590 (0.6), 646 (0.4). ^1H NMR [300 MHz, $CDCl_3$]: δ 9.04 (2 H, d, 2,6-pyridyl), 8.86 (8 H, m, pyrrole β), 8.22 (8 H, m, o-phenyl and 3,5-pyridyl), 7.77 (9 H, m, *m*- and *p*-phenyl), −2.83 (2 H, s, internal pyrrole).

***cis*-DPyTPP** [$C_{42}N_6H_{28}\cdot{}^1/_2H_2O$; fw = 625.76 g/mol]. Anal. Calcd: C, 80.62; N, 13.43; H, 4.67; O, 1.28. Found: C, 81.11; N, 13.49; H, 4.47; O, 0.81. Visible spectrum [λ, nm, in $CHCl_3$ ($\epsilon \times 10^4$, cm^{-1} M^{-1})]: 416 (22), 514 (1.8), 548 (0.7), 590 (0.6), 646 (0.3). ^1H NMR [300 MHz, $CDCl_3$]: δ 9.06 (4 H, d, 2,6-pyridyl), 8.86 (8 H, h, pyrrole β), 8.20 (8 H, m, *o*-phenyl and 3,5-pyridyl), 7.81 (6 H, m, *m*- and *p*-phenyl), −2.84 (2 H, s, internal pyrrole).

***trans*-DPyDPP** [$C_{42}N_6H_{28}\cdot H_2O$; fw = 633.77 g/mol]. Anal. Calcd: C, 79.48; N, 13.24; H, 4.76; O, 2.52. Found: C, 79.42; N, 12.83; H, 4.73; O, 2.53. Visible spectrum [λ, nm, in $CHCl_3$ ($\epsilon \times 10^4$, cm^{-1} M^{-1})]: 418 (23), 514 (1.0), 548 (0.4), 590 (0.3), 644 (0.2). ^1H NMR [300 MHz, $CDCl_3$]: δ 9.06 (4 H, d, 2,6-pyridyl), 8.90 (8 H, d, pyrrole β), 8.22 (8 H, m, *o*-phenyl, and 3,5-pyridyl), 7.79 (6 H, m, *m*- and *p*-phenyl), −2.86 (2 H, s, internal pyrrole).

TPyMPP [$C_{41}N_7H_{27}\cdot H_2O$; fw = 635.74 g/mol]. Anal. Calcd: C, 77.47; N, 15.42; H, 4.59; O, 2.51. Found: C, 77.90; N, 15.38; H, 4.29; O, 2.29. Visible spectrum [λ, nm, in $CHCl_3$ ($\epsilon \times 10^4$, cm^{-1} M^{-1})]: 418 (23), 514 (1.6), 548 (0.5), 590 (0.5), 644 (0.2). ^1H NMR [300 MHz, $CDCl_3$]: δ 9.07 (6 H, d, 2,6-pyridyl), 8.86 (8 H, m, pyrrole β), 8.18 (8 H, m, *o*-phenyl and 3,5-pyridyl), 7.80 (3 H, m, *m*- and *p*-phenyl), −2.90 (2 H, s, internal pyrrole).

The identities of TPP and TPyP were confirmed by visible spectroscopy and NMR spectroscopy.

TPP. Visible spectrum [λ, nm, in $CHCl_3$ ($\epsilon \times 10^4$, cm^{-1} M^{-1})]: 418 (25), 516 (1.8), 550 (0.77), 590 (0.54), and 646 (0.46). ^1H NMR [300 MHz, $CDCl_3$]: δ 8.86 (8 H, m, pyrrole β), 8.22 (8 H, m, *o*-phenyl), 7.78 (12 H, m, *m*- and *p*-phenyl), and −2.81 (2 H, s, internal pyrrole).

TPyP. Visible spectrum [λ, nm, in $CHCl_3$ ($\epsilon \times 10^4$, cm^{-1} M^{-1})]: 418 (20), 512 (1.3), 546 (0.37), 588 (0.40), 646 (0.14). ^1H NMR [300 MHz, $CDCl_3$]: δ 9.04 (8 H, d, 2,6-pyridyl), 8.82 (8 H, m, pyrrole β), 8.18 (8 H, m, 3,5-pyridyl), −2.95 (2 H, s, internal pyrrole).

Preparation of Zinc Monomers. Zinc(II) was inserted into the porphyrin monomers by standard methods.[15] An excess of zinc acetate (0.2500 g, 1.1 mmol) was added to 0.3870 g (0.63 mmol) of MPyTPP in 50 mL of DMF. The solution was refluxed for 1 h, after which a small sample of the reaction mixture was extracted and analyzed by using visible spectroscopy. The spectrum indicated that the metal insertion was complete, with the four Q bands of the free base (λ = 512, 550, 590, and 648 nm) collapsing to two peaks (λ = 560 and 602 nm). The DMF was then rotavaped off, and the zinc product was purified by using a 6 cm × 2.5 cm silica gel column with a chloroform/ethanol solvent system. The purple ZnMPyTPP powder was obtained in quantitative yield.

Zn^{II}MPyTPP. Visible spectrum [λ, nm, in $CHCl_3$ ($\epsilon \times 10^4$, cm^{-1} M^{-1})]: 422 (28), 564 (1.2), 606 (0.82). ^1H NMR [$CDCl_3$, 300 MHz]: d 8.86 (m, pyrrole β), 8.51 (m, pyrrole β), 8.10 (m, *o*-phenyl), 7.67 (m, *m*- and *p*-phenyl), 7.41 (m, pyrrole β), 6.23 (br, s, 3,5-pyridyl), 2.60 (br, s, 2,6-pyridyl).

When the zinc insertion reaction is performed on a larger scale with 1-g quantities of porphyrin monomer, an insoluble bright purple product is formed. The identity of this product was never determined; however, the possibility exists that this insoluble product is the tetrameric form of this oligomer.

Spectroscopic Measurements. All UV–visible spectra were obtained on a Hewlett-Packard 8451A diode-array spectrophotometer and plotted by a Hewlett-Packard 7470A plotter. ^1H NMR spectra were obtained on JEOL FX-90Q, Bruker WM-250, and Varian VXR-300 spectrometers at 90, 250, and 300 MHz, respectively. All fluorescence spectra were obtained from a Perkin-Elmer MPF-43A Fluorescence Spectrophotometer.

Crystal Structure Determination. A thin purple plate (0.38 × 0.14 × 0.03 mm) of $(C_{43}H_{27}N_5Zn)_n$ was obtained from crystallization from hot chloroform/methanol. The crystal was mounted on a glass fiber, and data were collected on a Syntex P3/F diffractometer. Mo Kα graphite-monochromatized radiation (λ = 0.71069 Å) was used in room-temperature (295 K) data collection. The cell dimensions were determined by a least-squares fit of 2θ for 25 reflections (15° ≤ 2θ ≤ 20°). Four standard reflections, 264, 42$\bar{1}$, $\bar{1}$32, and 021, were measured every 100 reflections with no significant variation. Intensities were obtained for 3 ≤ 2θ ≤ 35°, $\bar{1}$0 ≤ *h* ≤ 10, $\bar{1}$7 ≤ *k* ≤ 17, $\bar{1}$4 ≤ *l* ≤ 14, θ/2θ scans. A total of 13 230 reflections were collected, with 3152 unique reflections. R_{merge} was 0.0479. For $F_o > 6\sigma(R_o)$, there were 2130 observed reflections. Empirical absorption corrections were applied. Atomic scattering factors assumed were those taken from ref 16.

The zinc atom was located by using Patterson methods. The model was expanded by Fourier methods and refined by using block-cascade diagonal least-squares calculations. The function $\sum w(|F_o| - |F_c|)^2$ was minimized during cycles of the least-squares refinement. The weighting

(13) Adler, A. D.; Longo, F. R.; Finarelli, J. D.; Goldmacher, J.; Assour, J.; Korsalioff, L. *J. Org. Chem.* **1967**, *32*, 476.
(14) Hambright, P.; Williams, G. W.; Williams, R. F. X.; Lewis, A. *J. Inorg. Nucl. Chem.* **1979**, *14*, 41.
(15) Adler, A. D.; Longo, F. R.; Kampas, F.; Kim, J. *J. Inorg. Nucl. Chem.* **1970**, *2*, 2443.
(16) *International Tables for X-ray Crystallography*; Kynoch: Birmingham, England, 1974; Vol. IV.

Table I. Crystallographic Data for the ZnMPyTPP Polymer

formula: $C_{43}H_{27}N_5Zn$	V = 3348.16 (205) Å^3
FW = 678.4 (monomer)	Z = 4
space group: monoclinic, $P2_1/c$	ρ(calc) = 1.35 g/cm^3
a = 10.8392 (27) Å	T = 298 K
b = 19.1240 (85) Å	scan type; range: 2θ; 3–35°
c = 16.1580 (59) Å	R, R_w: 0.0626, 0.0732 (obsd data);
β = 90.326 (26)°	0.1045, 0.0901 (all data)

Table II. Zinc Porphyrin Visible Spectral Data

porphyrin	wavelength, nm	solvent
TPP	419, 516, 550, 590, 647	$CHCl_3$
ZnTPP	422, 548, 598	$CHCl_3$
ZnTPP(Py)	422, 556, 602	$CHCl_3$
ZnMPyTPP	422, 562, 606	$CHCl_3$

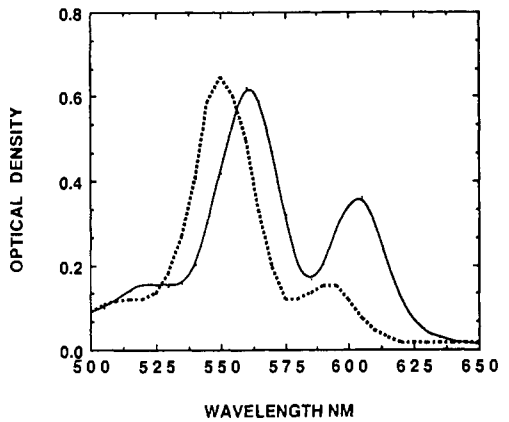

Figure 2. Visible spectrum of ZnMPyTPP in $CHCl_3$. (---) ZnMPyTPP at low concentration (1×10^{-5} M); ZnMPyTPP (—) at higher concentration (1×10^{-3} M)).

factor, w, was calculated from $w = 1.0/\{\sigma^2(F_o) + 0.0007(F_o^2)\}$. There were 322 least squares parameters. Positional and anisotropic parameters were refined for all non-H atoms. The H atoms were not included in the final model although several were observed in the final difference map. For the observed reflections, R = 0.0626 and R_w = 0.0732 where $R = \sum||F_o| - |F_c||/\sum|F_o|$ and $R_w = [\sum w(|F_o| - |F_c|)2/\sum w(F_o)^2]^{1/2}$. SHELXTL[17] programs were employed for the structure solution, refinement, and plotting. Pertinent crystallographic data are summarized in Table I; while a full table of crystallographic data and atomic structure factors are available as supplimentary materials.

Results and Discussion

ZnMPyTPP Polymer. Pyridine commonly binds to the metal center of metalloporphyrins.[18,19] The ZnMPyTPP polymer was formed by the coordination of a pyridine on the porphyrin periphery to an adjacent zinc metal center. The polymerization was confirmed by visible spectroscopy, fluorescence spectrophotometry, and proton NMR spectroscopy. The structure of the polymer was determined by X-ray crystallography and proton NMR spectroscopy.

The ZnMPyTPP visible spectrum showed the definite ligation of pyridine to the zinc porphyrin with Q bands undergoing a bathochromic shift characteristic of pyridine ligation to (5,10,15,20-tetraphenylporphyrinato)zinc(II) in chloroform.[19] Table II lists the absorption maxima for several zinc systems, and Figure 2 shows the visible spectrum for ZnMPyTPP.

Additionally, as the concentration of the monomer was increased a slightly greater bathochromic shift and an increased extinction coefficient was observed [602 nm (3200 M^{-1} cm^{-1}) to 606 nm (8500 M^{-1} cm^{-1})]. These spectral changes were attributed to polymerization.

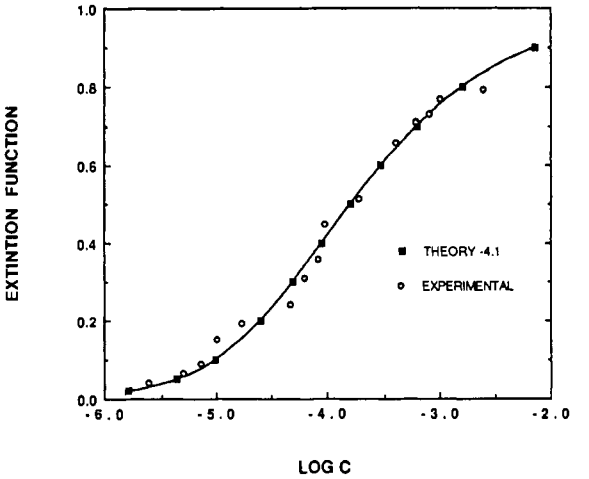

Figure 3. Statistical model for the polymerization of ZnMPyTPP [$(\epsilon - \epsilon_{mono})/(\epsilon' - \epsilon_{mono})$ vs log C]. The theoretical curve is shifted by log K =

Table III. Fluorescence Spectra for Zinc Systems

system	concn, M	Q(0–0), nm	Q(0–1), nm	I_1/I_2[a]
ZnTPP	6.6×10^{-5}	604	650	1.05
ZnTPP-py	6.6×10^{-5}	611	663	1.52
ZnMPyTPP	1.1×10^{-5}	603	649	1.30
	1.1×10^{-4}	614	652	1.23

[a] Ratio of intensities: $Q(0\text{–}0)/Q(0\text{–}1)$.

Furthermore, a statistical model for polymerization was developed, which demonstrated that the observed variations in extinction coefficients were indeed a result of polymerization in solution (derivation of the statistical model appears in the Appendix).

According to the model, a statistical relationship between equilibrium constants is assumed to exist; that is, if two monomers form a dimer with an equilibrium constant of κ, then an n-mer is formed from n monomers with an equilibrium constant of κ^{n-1}. If this statistical relationship exists, and if $\epsilon_n - \epsilon_{mono} = (n-1)\epsilon'$, then a correlation between original monomer concentration (C_{MP}) and extinction coefficient exists and can be expressed as

$$\epsilon - \epsilon_{mono} = (\epsilon' - \epsilon_{mono})\kappa C_{MP}(1 - \kappa[MP])^2 \qquad (1)$$

where ϵ_{mono} = monomer extinction coefficient, ϵ_n = n-mer extinction coefficient, ϵ = extinction coefficient of all coexisting species, and ϵ' = extinction coefficient of all coordinated porphyrin species. Plotting $(\epsilon - \epsilon_{mono})/(\epsilon' - \epsilon_{mono})$ vs log (κC_{MP}) revealed a good fit between the statistical model and the experimental results as demonstrated by Figure 3 and supported the premise that the ZnMPyTPP polymer was forming according to this statistical model. The equilibrium constant extracted from the data yield a value of 3.1×10^4, which is in the range for pyridine equilibrium constants with zinc porphyrins.[18,19]

The fluorescence spectra of ZnMPyTPP also indicated that coordination was occurring. Metalloporphyrins consisting of closed shell (d^{10}) metals generally fluoresce.[20] The luminescence of (5,10,15,20-tetraphenylporphyrinato)zinc(II) has been studied extensively.[21] Humphry-Baker and Kalyanasundaran have investigated the effects of various axial ligands, including pyridine, on the fluorescence of ZnTPP.[22] They reported that the coordination of the pyridine to the zinc metal center induces a red shift in the spectrum, as well as an increase in the relative intensities of the two emission bands [Q(0–0) (604 nm) vs Q(0–1) (660 nm)]. In this study, the fluorescence of ZnMPyTPP was explored in comparison to ZnTPP and ZnTPP-py. Table III lists the emission spectra for these systems. The emission spectra for ZnTPP and ZnTPP-py were consistent with the results in the literature.[22] At low concentration, the ZnMPyTPP shows an

(17) *SHELXTL*; X-ray Instruments Group, Nicolet Instrument Corp.: Madison, WI, 1985; Version 5.1.
(18) Smith, K. Ed. *Porphyrins and Metalloporphyrins*; Elsevier: New York, 1975.
(19) Dolphin, D., Ed. *The Porphyrins*; Academic: New York, 1978–1979; Vol. 1–7.
(20) Gouterman, M.; Seybold, P. G. *J. Mol. Spectrosc.* **1969**, *31*, 1.
(21) Harrinson, A. *J. Chem. Soc., Faraday Trans. 1* **1980**, *76*, 1978.
(22) Humphry-Baker, R.; Kalyanasundaran, K. *J. Photochem.* **1985**, *31*, 105.

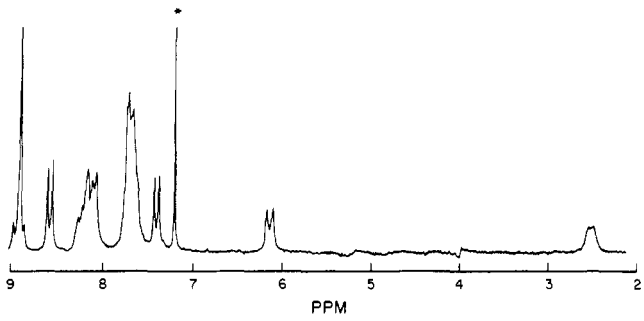

Figure 4. Proton NMR spectrum of ZnMPyTPP in $CDCl_3$.

Table IV. Atomic Coordinates ($\times 10^4$) and Thermal Parameters ($Å^2 \times 10^3$)

atom	x/a	y/b	z/c	U_{iso}[a]
Zn(1)	1553 (1)	1047 (1)	3124 (1)	44 (1)
N(1)	2699 (6)	1711 (3)	3785 (4)	41 (3)
N(2)	3033 (5)	800 (3)	2380 (4)	41 (3)
N(3)	629 (5)	178 (3)	2672 (4)	39 (2)
N(4)	298 (5)	1085 (3)	4070 (4)	27 (2)
N(5)	982 (6)	3167 (4)	7174 (4)	48 (2)
C(1)	2388 (7)	2083 (4)	4469 (5)	43 (3)
C(2)	3358 (8)	2573 (5)	4678 (6)	59 (4)
C(3)	4225 (8)	2491 (5)	4087 (6)	61 (4)
C(4)	3836 (7)	1949 (4)	3525 (5)	45 (3)
C(5)	4470 (7)	1719 (5)	2832 (5)	45 (3)
C(6)	4088 (7)	1189 (4)	2302 (5)	42 (3)
C(7)	4739 (8)	977 (5)	1574 (6)	60 (4)
C(8)	4107 (8)	463 (5)	1213 (6)	60 (4)
C(9)	2996 (7)	361 (4)	1717 (5)	44 (3)
C(10)	2048 (8)	−125 (4)	1546 (5)	40 (3)
C(11)	955 (8)	−218 (4)	2004 (5)	40 (3)
C(12)	20 (8)	−722 (4)	1822 (5)	47 (3)
C(13)	−874 (8)	−631 (4)	2383 (5)	47 (3)
C(14)	−520 (7)	−59 (4)	2916 (5)	39 (3)
C(15)	−1196 (7)	189 (4)	3575 (5)	34 (3)
C(16)	−798 (7)	726 (4)	4126 (5)	40 (3)
C(17)	−1497 (8)	1000 (5)	4810 (5)	51 (4)
C(18)	−819 (7)	1481 (5)	5183 (5)	50 (4)
C(19)	322 (7)	1544 (4)	4719 (5)	37 (3)
C(20)	1287 (7)	2001 (4)	4912 (5)	41 (3)

[a] Equivalent isotroic U defined as one-third of the trace of the orthogonalized U_{ij} tensor.

emission spectrum similar to ZnTPP. However, at a concentration of 1.1×10^{-4} M, the emission spectrum resembled that of ZnTPP-py with the ligation of the pyridine producing a red shift in the emission spectrum.

^{1}H NMR data on the polymer system also indicated that the pyridine on the porphyrin ring was bound to the zinc of another porphyrin (Figure 4). The resonances of the pyridine hydrogens in deutrochloroform occurred at 6.23 and 2.60 ppm and the pyrrole β-hydrogens appeared at 7.41, 8.51, and 8.86 ppm. For 5,10,15,20-tetrapyridylporphyrin, the pyrrole β-hydrogen resonances appeared as a singlet at 8.86 ppm while the pyridine resonances occurred at 9.04 and 8.22 ppm. Therefore, the ZnMPyTPP shifts indicate that both the pyridine and the pyrrole β-hydrogens were in the ring current of the porphyrin to which the 5-pyridyl-10,15,20-triphenylporphyrin is bound. A similar high-field shift was observed in the proton NMR of pyridine bound to (5,10,15,20-tetraphenylporphyrinato)zinc(II).[23] For the ZnTPP-py system, the pyridine proton shifts occurred at 2.66, 6.34, and 5.50 ppm (unbound pyridine 8.58, 7.62, and 7.21 ppm) with the pyrrole hydrogens equivalent. These ring current shifts are further explored later in this section.

Although the spectroscopic data strongly indicated that the polymer was indeed forming, the precise structure of the polymer was undetermined until an X-ray crystal structure was solved. Pertinent atomic coordinates are listed in Table IV. An ORTEP drawing of one of the monomeric units, 5-pyridyl-10,15,20-tri-

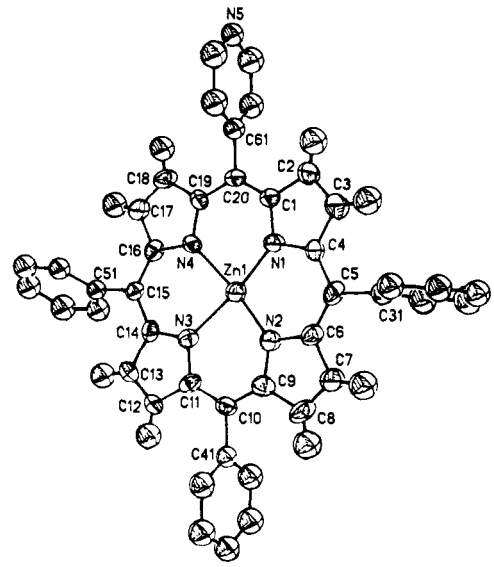

Figure 5. ORTEP of a ZnMPyTPP monomeric unit.

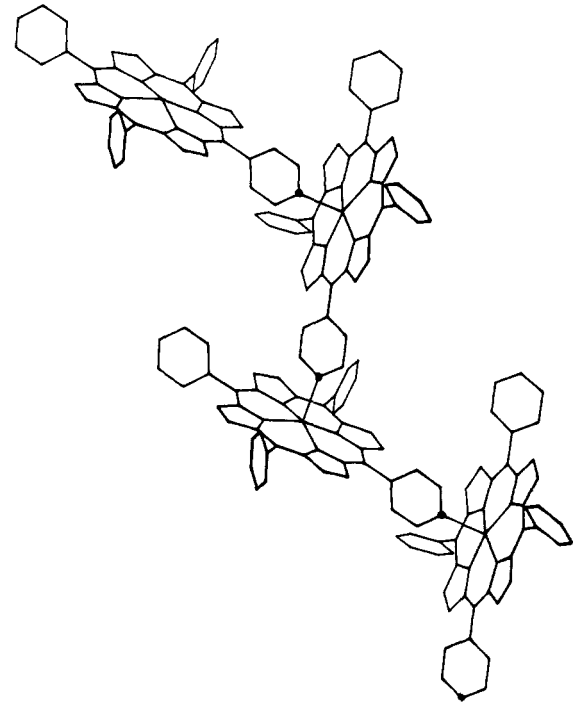

Figure 6. Polymeric structure of ZnMPyTPP.

phenylporphyrinato)zinc(II), appears in Figure 5. The long-chain polymeric crystal structure of ZnMPyTPP appears in Figure 6.

The zinc was 0.2849 out of the porphyrin plane, which is comparable to that found in other zinc porphyrins (0.2–0.3 Å).[19,24-28] The plane of the porphyrin displayed some ruffling of the pyrrole carbons, with deviations from the nitrogen plane ranging from 0.0028 to 0.2273 Å. The supplemenary materials contain these deviations.

The bond lengths and angles of the porphyrin monomer were similar to those of other porphyrin structures.[19,24] Selected bond lengths and angles appear in Table V. The Zn–N bond lengths were 2.069 (6), 2.066 (6), 2.070 (6), and 2.053 (6) Å, and the N–Zn–N bond angles were 88.5 (2), 89.3 (2), 89.6 (2), and 88.3

(23) Kirksey, C. H.; Hambright, P.; Stirm, C. B. *Inorg. Chem.* **1969**, *8*, 2141.
(24) Scheidt, W. R.; Lee, Y. T. In *Structure and Bonding*; Buchler, J. W., Ed.; Springer Verlag: Berlin, 1987; Vol. 64, pp 1–70.
(25) Collins, D. M.; Hoard, J. L. *J. Am. Chem. Soc.* **1970**, *92*, 3761.
(26) Margui, G.; Cammus, M.; Carta, G. *J. Coord. Chem.* **1973**, *2*, 167.
(27) Williams, G. J. B.; Andrews, L. C.; Spaulding, L. D. *J. Am. Chem. Soc.* **1977**, *99*, 6918.
(28) Cullen, D. L.; Meyer, E. F. *Acta Crystallogr., Ser. B* **1976**, *32*, 2259.

Table V. Selected Bond Lengths (Å) and Angles (deg)

Bond Length			
Zn(1)-N(1)	2.069 (6)	Zn(1)-N(4)	2.053 (6)
Zn(1)-N(2)	2.066 (6)	Zn(1)-N(5)[a]	2.234 (7)
Zn(1)-N(3)	2.070 (6)		
Bond Angle			
N(1)-N(1)-N(2)	88.5 (2)	N(1)-Zn(1)-N(5)	96.0 (3)
N(2)-Zn(1)-N(3)	89.3 (2)	N(3)-Zn(1)-N(5)	88.1 (2)
N(3)-Zn(1)-N(4)	88.3 (2)	N(3)-Zn(1)-N(5)	99.6 (2)
N(1)-Zn(1)-N(4)	89.6 (2)	N94)-Zn(1)-N(5)	107.8 (2)

[a] N(5) = pyridine nitrogen.

Table VI. Calculated[a,b] and Observed Ring Current Shifts (ppm) for the ZnTPP-Pyridine System

proton	calcd[a]	calcd[b]	obsd
a-py	-5.88	-5.90	-5.89
b-py	-1.76	-1.77	-1.76

[a] Abraham, R. J., et al. *Org. Magn. Reson.* **1980**, 418-424. [b] Our program—NMRSHIFT.

(2)°. The carbon–carbon and carbon–nitrogen bond lengths and angles were as expected.

Additionally, the zinc–pyridine bond length was 2.234 Å, slightly longer than similar zinc–pyridine bonds (2.0–2.2 Å) in other porphyrin structures.[19,25-28] Also, the zinc–pyridine bond was not perpendicular to the porphyrin plane, but instead was tilted 10° from the normal position. This tilted position has been observed in several other zinc–pyridine porphyrin structures, but not to the extent to which it occurred here.[27,28] Furthermore, the pyridine ring was tipped with respect to the Zn–N(py) bond; that is, the plane of the pyridine ring and the Zn–N(py) bond formed an angle of 155.6 (8)° rather than the expected 180°. This deviation is quite unusual for pyridine–porphyrin complexes.[24]

The extensive tilt of the bound porphyrin could have been the result of crystal-packing effects, but the possibility existed that the tilt was inherent to the polymeric structure in solution, as well as, in the solid state. Proton NMR spectroscopy was employed to investigate such a possibility.

The NMR spectra of porphyrins is dominated by ring current effects. These rings current effects are particularly prevalent in the ZnMPyTPP system in which the bound porphyrin protons experience a tremendous ring current effect and are greatly shifted up field.

Abraham and co-workers have developed a ring current model for porphyrins that allows the calculation of proton shifts which occur as a result of proximity to a porphyrin ring current.[29]

Abraham and co-workers have applied their porphyrin ring current model to investigate the solution geometry of $Zn^{II}TPP$ complexes with pyridine, 4-picoline, 2-picoline, quinoline, and isoquinoline substrates, as well as porphyrin aggregation.[30] Additionally, Chachaty has applied this theory to investigate the solution structure of carotenoporphyrins as chlorophyll models.[31] Abraham also developed similar ring current theories for chlorophyll derivatives and hydroporphyrins and implemented these to investigate chlorophyll aggregation and bacteriochlorophyllide *d* dimer geometry.[32]

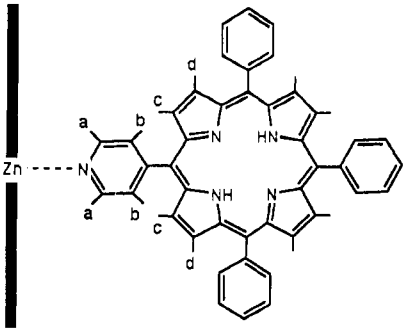

Figure 7. Proton identification for NMR shift calculations.

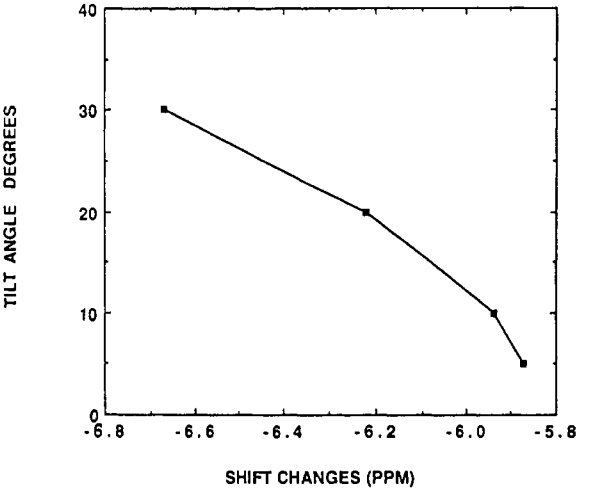

Figure 8. Predicted NMR ring current effect [tilt angle vs ring currents shifts] for pyridine proton a.

The porphyrin ring current theory was implemented to determine the solution structure of the one-dimensional ZnMPyTPP polymer. A computer program, NMRSHIFT,[33] was written as part of this study. The program allowed the calculation of ring current shifts based on Abraham's theory and ran in association with the CHEMX[34] molecular-modeling program on a microVAX computer system.

Generally, a particular molecular configuration was assembled by using CHEMX. An atomic coordinate file was then created, which was read by NMRSHIFT. The ring current shifts were calculated by NMRSHIFT and output in a designated file and stored either in a given directory or on magnetic tape.

For the ZnMPyTPP system, a monomeric porphyrin structure was read by CHEMX. A second monomeric structure was then read into CHEMX and joined to the first through a bond between the metal center of the first monomer and the nitrogen of a pyridine ring on the periphery of the second. The atomic coordinates of these porphyrins were read by NMRSHIFT, which calculated the ring current effect on each of the protons of the bound porphyrin. The shifts are rotationally averaged values; that is, the M–N(py) bond was rotated at increments of 10°, and the shifts were calculated for each position and averaged. Table VI displays the NMRSHIFT results of this calculation for the pyridine protons as well as Abraham's results for a similar system. The results calculated by NMRSHIFT were in good agreement with Abraham's work, as well as, experimental results.

The experimental NMR data indicated that not only the pyridine protons but also the pyrrole β-protons were affected by the adjacent ring current. Figure 7 identifies the porphyrin protons of interest. The a, b, c, and d protons of Figure 8 were the protons

(29) (a) Abraham, R. *J. Mol. Phys.* **1961**, *4*, 145. (b) Abraham, R. J.; Fell, S. C. M.; Smith, K. M. *Org. Magn. Reson.* **1977**, *9*, 367. (c) Abraham, R. J.; Bedford, G. R.; McNeillie, D.; Wright, B. *Org. Magn. Reson.* **1980**, *14*, 418.

(30) (a) Abraham, R. J.; Bedford, G. R.; Wright, B. *Org. Magn. Reson.* **1982**, *18*, 45. (b) Abraham, R. J.; Smith, K. M. *J. Am. Chem. Soc.* **1983**, *105*, 5734.

(31) Chachaty, C.; Gust, D.; Moore, T. A.; Nemeth, G. A.; Liddell, D. A.; Moore, A. L. *Org. Magn. Reson.* **1984**, *22*, 39.

(32) (a) Abraham, R. J.; Smith, K. M.; Goff, D. A.; Bobe, F. W. *J. Am. Chem. Soc.* **1985**, *107*, 1085. (b) Abraham, R. J.; Medforth, C. J.; Smith, K. M.; Goff, D. A.; Simpson, D. J. *J. Am. Chem. Soc.* **1987**, *109*, 4786. (c) Smith, K. M.; Bobe, F. W.; Goff, D. A.; Abraham, R. J. *J. Am. Chem. Soc.* **1986**, *108*, 1111. (d) Abraham, R. J.; Smith, K. M.; Goff, D. A.; Lai, j. *J. Am. Chem. Soc.* **1982**, *104*, 4332. (e) Smith, K. M.; Goff, D. A.; Abraham, R. J.; Plant, J. E. *Org. Magn. Reson.* **1983**, *21*, 505.

(33) Shachter, A. M. *Coordinated and Linked Porphyrin Dimers, Trimers, and Polymers.* Ph.D. Dissertation, University of Colorado, Boulder, CO, 1989.

(34) CHEM-X is developed and distributed by Chemical Design Ltd., Oxford, England.

Table VII. Calculated and Experimental Ring Current Shifts for ZnMPyTPP (ppm)

proton	exptl	calcd(25)[a]	calcd(0)[a]
a-H	−6.4 ppm	−6.45	−5.88
b-H	−1.9	−1.59	−1.78
c-H (pyrrole β)	−1.3	−1.16	−1.28
d-H (pyrrole β)	−0.3	−0.38	−0.44

[a] Tilt angle (deg) given in parentheses.

Table VIII. Visible Spectra Data for Porphyrin Monomers and ZnTPP Dimer and Trimers (in $CHCl_3$)

porphyrin system	wavelength, nm	I_{550}/I_{516}
monomers		
ZnTPP	548, 598	
MPyTPP	516, 550, 590, 646	0.41
cis-DPyDPP	514, 548, 590, 646	0.39
trans-DPyDPP	514, 548, 590, 644	0.40
dimer		
ZnTPP + 2MPyTPP	516, 550, 592, 646	1.25
trimers		
2ZnTPP + *cis*-DPyDPP	516, 550, 592, 644	1.69
2ZnTPP + *trans*-DPyDPP	514, 550, 592, 644	1.82

noticably affected by the adjacent ring current and were consequently the focus of this study.

Table VII lists the NMRSHIFT results for the pyrrole β (c, d) and the pyridine (a, b) protons for a 5-pyridyl-10,15,20-triphenylporphyrin ligand of the polymeric porphyrin. Additionally, the experimental NMR shift results for ZnMPyTPP and the NMRSHIFT results for the crystalo structure appear in Table VII. CHEMX and NMRSHIFT were used to investigate the effects of tilt angle on the NMR ring shifts.

Using tilt angles of 10, 20, and 30° ring current effects were calculated. Figure 8 shows the effect of tilt angle on the shifts of the a pyridine protons. The tilt data calculated by using NMRSHIFT indicate that a tilt angle of 25° generates shifts that are similar to those found experimentally (Table VII). Hence, the polymer structure in solution and in a solid state have unique pyridine bonding characteristics with the pyridine ring tilted extensively.

Dimer and Trimers. Pyridine meso-substituted porphyrins were used to axially coordinate to metalloporphyrins, thereby forming dimeric and trimeric systems. Specifically, the coordination of one molecule of 5-pyridyl-10,15,20-triphenylporphyrin to the zinc center of (5,10,15,20-tetraphenylporphyrinato)zinc(II) (ZnTPP) created a coordinated dimer and the coordination of the two pyridine rings of 5,10-dipyridyl-15,20-diphenylporphyrin or 5,15-dipyridyl-10,20-diphenylporphyrin with two different ZnTPP molecules created a trimer. The formation of these oligomers was confirmed by spectroscopic methods.

The visible spectra of these oligomeric systems are listed in Table VIII. These oligomer spectra were simply a composite of the absorptions of both the ZnTPP and the free-base ligands. The coordination of the pyridine on the porphyrin periphery to the zinc metal center generally would induce a red shift in the bound ZnTPP spectrum; however, due to the overlapping nature of the absorption spectra, the pyridine coordination could not be confirmed.

The proton NMR spectra of these systems did show definite evidence of coordination. The proton NMR showed resonances of bound MPyTPP. The bound pyridine protons were shifted upfield by the ZnTPP ring current and appear at 4.68 and 6.89 ppm. The pyrrole β-protons of MPyTPP also showed ring current effects as they were split with shifts of 7.89, 8.59, and 8.79 ppm (the pyrrole β-protons are generally a singlet at 8.86 ppm in free-base porphyrins). The phenyl protons of MPyTPP appeared as expected at 8.08 and 7.70 ppm. Consequently, the upfield shifts of the pyridine and pyrrole β-protons as a result of the ZnTPP ring current confirmed that the dimer was forming.

The trimers showed similar proton NMR shifts with the bound *cis*-DPyDPP of the 2ZnTPP + *cis*-DPyDPP trimer resonances appearing at 8.65, 8.49, and 7.45 for the pyrrole β-protons, 3.96 and 6.56 for the pyridine protons, and 7.95 and 7.77 for the *o*-, *m*-, and *p*-phenyl protons. These shifts indicated that the pyridine rings were bound to the zinc metal centers and, therefore, experienced a tremendous ring current effect, causing the pyridine resonances, as well as the β-pyrrole resonances, to be shifted upfield. Thus, the NMR spectra of these systems indicated that the dimer and trimers were formed in solution. The proposed structure of the trimer appears in Figure 9.

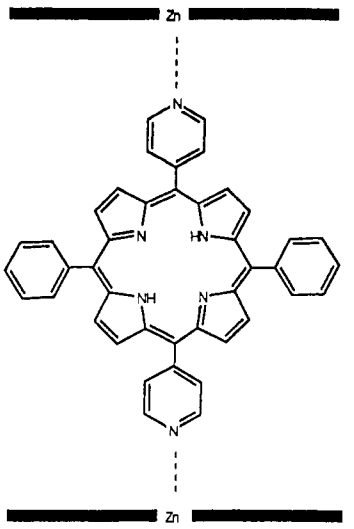

Figure 9. Proposed trimer structure.

Conclusion

In this paper, the spectroscopic and structural properties of metalloporphyrin oligomers and a polymer were presented. The formation of the ZnMPyTPP polymer was described by a statistical model for polymerization. The X-ray crystal structure of the ZnMPyTPP polymer revealed that the pyridine was bound to the zinc with an unsual tilt, presumably the result of strain induced by polymerization.

NMRSHIFT, a program written for this study, calculated NMR ring current effects, which indicated that the structures of the ZnMPyTPP-coordinated polymer were similar both in solution and in the solid state.[35]

Acknowledgment. We thank Edward King for his help in the derivation of the statistical model, R. Curt Haltiwanger for his help in the crystal structure determination, and Jan Giovannettii for her synthetic and chromatographic contributions.

Appendix

Derivation of Statistical Model For Polymerization. If $2AX \rightarrow (AX)_2$ with $K = \kappa$ and $3AX \rightarrow (AX)_3$ with $K = \kappa^2$ then $nAX \rightarrow (AX)_n$ with $K = \kappa^{n-1}$. If this statistical relationship between equilibrium constants exists and if $\epsilon_n - \epsilon_{monomer} = (n-1)\epsilon'$, then

$$\epsilon = \sum \epsilon_n[(AX)_n]/\sum n[(AX)_n] \quad (2)$$

$$\epsilon = \sum \epsilon_n \kappa^{n-1}[AX]^n/\sum n\kappa^{n-1}[AX]^n \quad (3)$$

$$\epsilon = \frac{\sum(\epsilon_{monomer} + (n-1)\epsilon')\kappa^{n-1}[AX]^n}{\sum n\kappa^{n-1}[AX]^n} \quad (4)$$

$$\epsilon = \frac{[AX]\sum(\epsilon_{monomer} + (n-1)\epsilon')\kappa^{n-1}[AX]^{n-1}}{[AX]\sum n\kappa^{n-1}[AX]^{n-1}} \quad (5)$$

$$\epsilon - \epsilon_{monomer} = \frac{\sum \kappa^{n-1}[AX]^{n-1}(\epsilon_{monomer} + (n-1)\epsilon' - n\epsilon_{monomer})}{\sum n\kappa^{n-1}[AX]^{n-1}} \quad (6)$$

(35) Higher order polymers of (5-pyridyl-10,15,20-triphenylporphyrinato)-cobalt(III), (5-pyridyl-10,15,20-triphenylporphyrinato)iron(II), 5,10-dipyridyl-15,20-diphenylporphyrinato)cobalt(III), and 5,15-dipyridyl-10,20-diphenylporphyrinato)cobalt(III) were also studied. Structural characterization of these polymers was limited by the insolubility of these systems.

Expanding the series gives

$$\epsilon - \epsilon_{monomer} = \frac{\kappa[AX](\epsilon' - \epsilon_{monomer}) + \kappa^2[AX]^2(2(\epsilon' - \epsilon_{monomer}) + \ldots}{1 + 2\kappa[AX] + 3\kappa^2[AX]^2 + \ldots} \quad (7)$$

$$\epsilon - \epsilon_{monomer} = (\epsilon' - \epsilon_{monomer}) \frac{\kappa[AX](1 + 2\kappa[AX] + 3\kappa^2[AX]^2) + \ldots}{1 + 2\kappa[AX] + 3\kappa^2[AX]^2 + \ldots} \quad (8)$$

$$\epsilon - \epsilon_{monomer} = \kappa[AX]\ (\epsilon' - \epsilon_{monomer}) \quad (9)$$

Correlating to the total monomer concentration gives $C_{AX} = \sum n[(AX)_n]$, where

$$C_{AX} = [AX]\sum n\kappa^{n-1}[AX]^{n-1} = [AX]/(1 - \kappa[AX]^2) \quad (10)$$

Substituting this expression into eq 9 leads to

$$\epsilon - \epsilon_{monomer} = (\epsilon' - \epsilon_{monomer})\kappa C_{AX}\ (1 - \kappa[AX])^2 \quad (11)$$

Supplementary Material Available: Tables S1–S6, listing atomic coordinates, thermal parameters, bond lengths, bond angles, deviations of atoms from the porphyrin plane, and crystal data collection parameters (8 pages); Table S7, listing observed and calculated structures factors (19 pages). Ordering information is given on any current masthead page.

Notes

Contribution from the Inorganic Chemistry Laboratory, University of Oxford, South Parks Road, Oxford OX1 3QR, U.K.

Size and Shape Characteristics of Inorganic Molecular Ions and Their Relevance to Crystallization Problems

D. Michael P. Mingos* and Andrew L. Rohl

Received January 3, 1991

The crystallization of molecular salts in coordination and organometallic chemistry has always been a critical step in the characterizational process because of the requirement for single crystals suitable for diffraction studies. Despite the general importance of this process, it has been little studied either from an experimental or theoretical point of view. Inorganic chemists have at their disposal a range of cations and anions with varying, but ill-defined, sizes and solubility properties and by a process of trial and error attempt to obtain crystals with the desired solubility properties and morphology. If inorganic chemists are to transform this "art" into procedures that enable them to truly design and fine tune at a molecular level those solid-state properties which have been defined as important, such as conductivity,[1] magnetic ordering,[2] and nonlinear optical properties,[3,4] then it will be necessary to understand in more detail the experimental and theoretical factors governing the crystallization process and organization of molecules in a crystal. This paper provides a tentative first step toward this goal by providing data on the molecular volumes, surface areas, and shapes of a wide range of ions used in coordination chemistry.

Basolo[5] has pioneered attempts to systematize the requirements for crystallizing coordination compounds with unusual geometries and coordination numbers. He proposed the empirical observation that "*Solid salts separate from aqueous solution easiest for combinations of either small cation-small anion or large cation-large anion, preferably with systems having the same but opposite charges on the counterions*". Further examples of this phenomenon have been cited by McDaniel.[6] The requirement of matching small cations and anions and large cations and anions has therefore passed into the folklore of inorganic chemistry but has not been substantiated by quantitative criteria. McDaniel has analyzed the role of large countercations based on his concept of "lattice inhibited" reactions. Using simple Born theory, he concluded, in contrast to Basolo's size-matching rule, that there is a lower critical limit for the size of the cation but no upper limit. Recently we have calculated the molecular volumes (V_m), surface areas (S_m), and shapes of a wide range of cations and anions, and the results are given in Tables I and II. The method used to calculate the volume is that of Gavezzotti.[7] The molecular volume is calculated by sampling a parallelepiped, which contains an ion constructed from van der Waals spheres centered on the atomic positions, with a large number of probe points (N) and counting the number (N_{occ}) of points inside at least one of the van der Waals

Table I. Size and Shape Parameters of Some Common Inorganic and Organometallic Cations

cation	V_m, Å^3	S_m, Å^2	F_s	F_c	F_d
Li^+	2	8			
Na^+	3	12			
K^+	10	22			
Cs^+	19	34			
$[NH_4]^+$	24	43	1.00	0.00	0.00
$[NH_3Me]^+$	41	64	0.39	0.61	0.44
$[NMe_4]^+$	91	123	1.00	0.00	0.00
$[Pt(NH_3)_4]^{2+}$	99	142	0.12	0.44	0.88
$[dienH_3]^+$	108	148	0.04	0.94	0.93
$[Cr(NH_3)_6]^{3+}$	126	176	0.93	0.07	0.04
$[Co(NH_3)_4(NO_2)_2]^+$	134	191	0.84	0.10	0.14
$[Me_2NHCH_2CH_2NHMe_2]^+$	140	182	0.09	0.81	0.85
$[Fe(\eta\text{-}C_5H_5)(CO)_3]^+$	140	166	0.83	0.15	0.11
$[Fe(\eta\text{-}C_5H_5)_2]^+$	145	168	0.56	0.44	0.29
$[Hg(en)_2]^{2+}$	150	195	0.12	0.81	0.81
$[NEt_4]^+$	156	183	0.35	0.33	0.65
$[NBu_2H_2]^+$	157	206	0.09	0.87	0.85
$[Cr(\eta\text{-}C_6H_6)_2]^{3+}$	175	196	0.79	0.21	0.13
$[Cr(en)_3]^{3+}$	192	236	0.38	0.32	0.61
$[Co(pn)_3]^{3+}$	253	317	0.39	0.30	0.61
$[Cr(tn)_3]^{3+}$	256	303	0.39	0.38	0.58
$[PPh_3Me]^+$	271	310	0.39	0.32	0.60
$[AsPh_3Me]^+$	278	311	0.49	0.25	0.51
$[NBu_4]^+$	287	346	0.14	0.43	0.86
$[Fe(\eta\text{-}C_5Me_5)_2]^+$	309	362	0.89	0.06	0.11
$[PPh_4]^+$	317	349	0.90	0.08	0.07
$[AsPh_4]^+$	334	364	0.82	0.09	0.17
$[Co(PMe_3)_4]^{3+}$	338	425	0.83	0.16	0.10
$[Co(\eta\text{-}C_6Me_6)_2]^+$	361	397	0.81	0.10	0.19
$[Fe_4(\eta\text{-}C_5H_5)_4(\mu^3\text{-}S)_4]^+$	384	390	0.57	0.36	0.33
$[Ni(bpy)_3]^{3+}$	448	483	0.88	0.08	0.09
$[Ni_6(\eta\text{-}C_5H_5)_6]^+$	470	504	1.00	0.00	0.00
$[Ni(phen)_3]^{3+}$	485	514	0.60	0.26	0.36
$[PPN]^+$	490	543	0.70	0.27	0.20
$[Au(PPh_3)_3]^+$	761	836	0.60	0.23	0.38
$[Au(PPh_2Me)_4]^+$	795	879	0.78	0.22	0.12

(1) Williams, J. M.; Wang, H. H.; Emge, T. J.; Geiser, U.; Beno, M. A.; Leung, P. C. W.; Carlson, K. D.; Thorn, R. J.; Schultz, A. J.; Whangbo, M. H. In *Progress in Inorganic Chemistry*; Lippard, S. J., Ed.; John Wiley & Sons Inc.: New York, 1987; Vol. 35, pp 51–218.
(2) Miller, J. S.; Epstein, A. J.; Reiff, W. M. *Acc. Chem. Res.* **1988**, *21*, 114.
(3) Tam, W.; Calabrese, J. C. *Chem. Phys. Lett.* **1988**, *144*, 79.
(4) Green, M. L. H.; Marder, S. R.; Thompson, M. E.; Bandy, J. A.; Bloor, D.; Kolinsky, P. V.; Jones, R. J. *Nature* **1987**, *330*, 360.
(5) Basolo, F. *Coord. Chem. Rev.* **1968**, *3*, 213.
(6) McDaniel, D. H. *Annu. Rep. Inorg. Gen. Synth.* **1972**, 293.
(7) Gavezzotti, A. *J. Am. Chem. Soc.* **1983**, *105*, 5220.

0020-1669/91/1330-3769$02.50/0